Inverse Prism based on Temporal Discontinuity and Spatial Dispersion

Alireza Akbarzadeh,* Nima Chamanara, and Christophe Caloz

Polytechnique Montréal, Montréal, QC H3T 1J4, Canada

(Dated: March 4, 2019)

In duality with the general functionality of a conventional prism and its universal properties, an inverse prism is introduced. On account of the momentum continuity at a purely temporal interface, it is shown that instantaneous switching of an isotropic medium to an anisotropic medium leads the incident frequency to refract like a vectorial field —a counterintuitive property, which is the basis of the inverse prism mechanism. Through the analysis of the dispersion diagrams before and after the temporal transition, the concepts of inhomogeneous frequency refraction and frequency birefringence are explained, and in this regard a Snell law like formulation is given. Furthermore, it is shown that by crossing the inverse prism interface the polarization vector of a plane wave traces the Lissajous curves —an unusual feature which can be employed to manipulate the spin-orbit interaction of the structured light.

PACS numbers: 42.79.Bh, 42.65.Sf

An optical prism, represented in Fig. 1(a), is a transparent device, which decomposes incident white light into its constituent colors by refracting them into different directions. This phenomenon was previously believed to result from the production of colors by the prism, and it is Newton who first found out, experimentally, that it was rather due to the decomposition of the colors already present in the incoming light. Newton later explained in his book Opticks [1] that spectral decomposition itself results from the frequency dispersive nature of the glass medium forming the prism, whereby the refractive index is a function of frequency. From a mathematical perspective, one may consider a prism as a device that maps temporal frequencies (ω) into spatial frequencies ($\mathbf{k}$), as shown in Fig. 1(b).

In this paper, we raise the question as to whether it may be possible to accomplish the inverse operation to that of the prism, namely mapping spatial frequencies into temporal frequencies, as mathematically suggested in Fig. 1(d). What would that physically mean? Reading out Fig. 1(d) from a physical perspective leads to the physical operation depicted in Fig. 1(c): waves with different directions but identical frequency would transform into waves with different frequencies without change of direction. A device performing this operation would naturally be referred to as an *inverse prism*.

How could such an inverse prism be practically realized? Comparing Figs. 1(b) and 1(d), as well as Figs. 1(a) and 1(c), reveals that the inverse operation results from swapping space and time. The conventional and inverse prisms are thus the *space-time dual* of each other. This consideration should naturally lead us to the realization of the inverse prism.

A conventional prism is characterized by a) broken spatial symmetry [$n = n(\mathbf{r})$], which results in alteration (non-conservation) of the momentum of light, leading to spatial refraction, and b) frequency dispersion [$n_2 = n_2(\omega)$], typically present in glass materi-
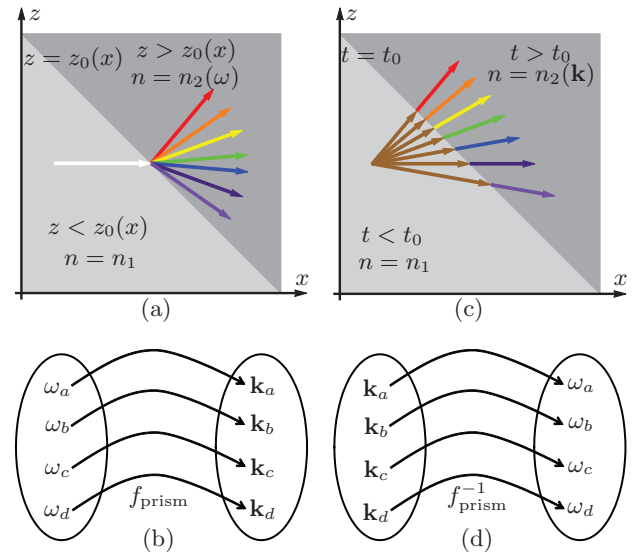

FIG. 1: Comparison of the conventional prism and the inverse prism, formed by the refractive indices n_1 and n_2 with $n_2 > n_1$. (a) Conventional prism, decomposing white light into its constituent colors, using spatial discontinuity [$n = n(\mathbf{r})$] and temporal dispersion [$n_2 = n_2(\omega)$]. (b) Corresponding mapping from temporal frequencies (ω) to spatial frequencies ($\mathbf{k}$). (c) Inverse prism, transforming multidirectional light into direction-dependent new colors, using temporal discontinuity [$n = n(t)$] and spatial dispersion [$n_2 = n_2(\mathbf{k})$]. (d) Corresponding mapping from spatial to temporal frequencies.

als at optical frequencies, to refract different frequencies into different directions. Therefore, the inverse prism should be characterized by a') broken temporal symmetry [$n_2 = n_2(t)$], resulting in alteration (non-conservation) of the energy, or frequency of light and *temporal refraction* [2, 3], and b') spatial dispersion [$n_2 = n_2(\mathbf{k})$], for which a proper mechanism is to be devised to "refract" different directions (spatial frequencies) into different (temporal) frequencies. Thus, these

dual properties constitute the key requirements to realize an inverse prism.

The first requirement, broken temporal symmetry [a′] above], can be accomplished by incorporating instantaneous (step-like) *time switching* between two different media. Such temporal switching may be implemented by ionizing plasmas [4, 5], exciting nonlinearities [6], producing shock waves [7, 8] or modulating varactors [9]. The electrodynamics of wave propagation and light-matter interaction in temporal media and, in general, switched media have been well studied in past decades. In the late 1960ies, Morgenthaler solved the problem of light propagation in dielectric media with time varying wavenumbers, with specific application to step and sinusoidal temporal modulations [10]. About a decade later, his work was extended to time-varying media that are dispersive and include electromagnetic sources by Felsen and Whitman [11], and to scattering by a spatial interface between vacuum and time-varying dielectric or dispersive media by Fante [12]. From the 1970ies to the turn of the 20$^\text{th}$ century, studies of switched media were mostly restricted to plasma physics [4, 5] and nonlinear optics [6]. However, there has recently been a general regain of interest in the electrodynamics of light-matter interactions, in the context of temporal resonators and waveguides [13–16], photonic crystals with spatiotemporal defects [7, 8, 17], space-time modulated graphene sheets [18], and spatiotemporal metasurfaces [19].

The second requirement for realizing an inverse prism, spatial dispersion [b′] above], can be fulfilled by performing the aforementioned time switching from a standard isotropic medium (n_1) to an *anisotropic* medium ($\bar{\bar{n}}_2$), which may alternatively be seen as the time-varying medium

$$n(t) = n_1 u(t_0 - t) + \bar{\bar{n}}_2 u(t - t_0), \qquad (1)$$

where $u(\cdot)$ is the step function and t_0 is the switching time. We shall consider here the typical optical case of non-magnetic materials, where $\mu_1 = \mu_2 = \mu_0$ and $n_1 = \sqrt{\epsilon_1/\epsilon_0}$, $n_{2,ij} = \sqrt{\epsilon_{2,ij}/\epsilon_0}$ with $i, j = \{1, 2, 3\}$.

The anisotropic medium $\bar{\bar{n}}_2$, which may be generally characterized by the constitutive susceptibility tensor $\bar{\bar{\chi}} = \chi_{ij}$, is intrinsically spatially dispersive since its dispersion relation, $\omega = g(\chi_{ij}, \mathbf{k})$ [20–22], can be alternatively written as $\omega = ck_0/n(\mathbf{k})$ with $n(\mathbf{k}) = ck_0/g(\chi_{ij}, \mathbf{k})$ and $k_0 = \omega/c$ being the vacuum wavenumber associated with the vacuum speed c. In this paper, for simplicity but without loss of generality, we consider the case of uniaxial anisotropy, with the optical axis parallel to the z axis and the refractive index tensor $\bar{\bar{n}} = \text{diag}\{n_\parallel, n_\parallel, n_\perp\}$, as indicated in Fig. 2(a). This anisotropy allows one to decompose the problem into s (out-of-plane or TE or ordinary) polarization and p (in-plane or TM or extraordinary) polarization, as shown in the inset of the same figure.
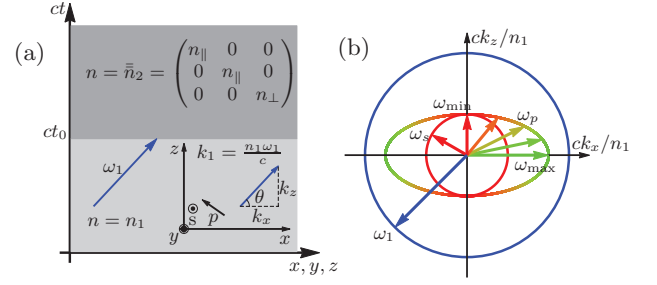

FIG. 2: Implementation of the inverse prism in Figure 1(c) and (d), as the time-varying medium described by (1). (a) Space-time representation of the inverse prism, whose anisotropy, here uniaxial, induces birefringence, with inset showing the xz space, the s, p polarizations and the angle of wave propagation θ. (b) Circular (isotropic) and elliptical (anisotropic) isofrequency curves corresponding to (3) and (6), respectively, for $n_1 < n_\perp < n_\parallel$.

Note that, the switching from medium n_1 to medium $\bar{\bar{n}}_2$ in (1), being purely temporal, incurs no change in spatial frequencies, i.e. $\mathbf{k}_2 = \mathbf{k}_1 = \mathbf{k}$: it is the momentum ($\mathbf{k}$) that is conserved in a temporal discontinuity problem [16, 23, 24]. This contrasts with the conservation of frequency (ω) or energy ($\hbar\omega$) in a spatial discontinuity problem. Thus, the angle of propagation is not affected by the discontinuity, i.e. $\theta_2 = \theta_1 = \theta$.

Let us consider a harmonic incident plane wave with angular frequency ω_1 propagating in the $x-z$ plane of the earlier isotropic medium ($n = n_1$, $t < t_0$) under the angle θ with respect to the x axis, as illustrated in Fig. 2(a). The corresponding dispersion relation may be written as

$$k_1 = n_1\frac{\omega_1}{c} = \sqrt{k_x^2 + k_z^2} \quad \text{or} \quad \omega_1 = \frac{c}{n_1}\sqrt{k_x^2 + k_z^2}, \quad (2)$$

where k_x and k_z are the x and z components of wave vector $\mathbf{k}$, respectively. This relation describes a circle with radius ω_1 in the isofrequency diagram normalized to n_1/c, as plotted in blue in Fig. 2(b).

In the s-polarization problem, with electric field directed along the y direction, the later medium is seen as purely isotropic, with refractive index $n_2 = \sqrt{\epsilon_\parallel/\epsilon_0} = n_\parallel$. Therefore, accounting also for momentum conservation, the later dispersion relation is identical to (2) with n_1 replaced by $n_\parallel$, i.e.

$$k_\text{s} = n_\parallel\frac{\omega_\text{s}}{c} = \pm\sqrt{k_x^2 + k_z^2} \quad \text{or} \quad \omega_\text{s} = \pm\frac{c}{n_\parallel}\sqrt{k_x^2 + k_z^2}, \quad (3)$$

corresponding to the smaller circle in the isofrequency diagram of Fig. 2(b), where the $+$ and $-$ denote the transmitted (forward) and reflected (backward) wave in the later medium with respective scattering coefficients, T_s and R_s, as [23, 24]

$$T_\text{s} = \frac{\omega_\text{s} + \omega_2}{2\omega_1}, \qquad (4)$$

$$R_{\mathrm{s}} = \frac{\omega_{\mathrm{s}} - \omega_2}{2\omega_1}. \qquad (5)$$

The p-polarization problem, which is of greater interest, is more complex and the corresponding dispersion relation is

$$n_{\parallel}^2 n_{\perp}^2 k_0^2 = n_{\parallel}^2 n_{\perp}^2 \left(\frac{\omega_{\mathrm{p}}}{c}\right)^2 = n_{\parallel}^2 k_x^2 + n_{\perp}^2 k_z^2 \quad \text{(6a)}$$

which becomes, upon dividing by $n_{\parallel}^2 n_{\perp}^2/c^2$ and taking the square root,

$$\omega_{\mathrm{p}} = \omega_{\perp} = \pm\sqrt{\left(\frac{c}{n_{\perp}}\right)^2 k_x^2 + \left(\frac{c}{n_{\parallel}}\right)^2 k_z^2}, \qquad (6b)$$

where the $+$ and $-$ denote again the transmitted (forward) and reflected (backward) wave in the later medium with respective scattering coefficients, T_{p} and R_{p}, that may be straightforwardly found by enforcing continuity of the $\mathbf{D}$ and $\mathbf{H}$ fields at $t = t_0$,

$$T_{\mathrm{p}} = \frac{n_1^2 \sqrt{n_{\perp}^4 k_z^2 + n_{\parallel}^4 k_x^2}}{n_{\parallel}^2 n_{\perp}^2 \sqrt{k_x^2 + k_z^2}} \left(\frac{\omega_1 + \omega_p}{2\omega_1}\right), \qquad (7)$$

$$R_{\mathrm{p}} = \frac{n_1^2 \sqrt{n_{\perp}^4 k_z^2 + n_{\parallel}^4 k_x^2}}{n_{\parallel}^2 n_{\perp}^2 \sqrt{k_x^2 + k_z^2}} \left(\frac{\omega_1 - \omega_p}{2\omega_1}\right). \qquad (8)$$

The relation (6b) describes an ellipse with major and minor semi-axes $\omega_{\max} = (n_1/n_{\perp})\omega_1$ and $\omega_{\min} = (n_1/n_{\parallel})\omega_1 = \omega_{\mathrm{s}}$, respectively, as plotted in gradient color in Fig. 2(b). Thus, the scattered frequency is a function of the wave direction, or $\omega = \omega(\mathbf{k})$, which corresponds to the sought after inverse prism operation [Fig. 1(c) and (d)].

We have just considered the s-polarization and p-polarization problems separately. However, a general wave, as for instance unpolarized light, may carry both polarizations. Such a hybrid wave would be split by the anisotropic inverse prism of Fig. 2 into an s-wave and a p-wave seeing the frequency transformations (3) and (6), respectively. The prism thus exhibits temporal frequency birefringence, specifically *chromatic refraction birefringence*, which is a type of birefringence not found in structures with spatial discontinuities or isotropic temporal discontinuities. This birefringence phenomenon is illustrated in Fig. 3. Monochromatic light rays with identical frequency, ω_1, propagating in different directions in the earlier medium are scattered without change of direction as modified monochromatic and polychromatic waves for the s-polarization and p-polarization cases, respectively.

Another interesting perspective of the inverse prism is that it bears *analogy with Snell law* of refraction at a spatial discontinuity. For the case of s-polarization in the
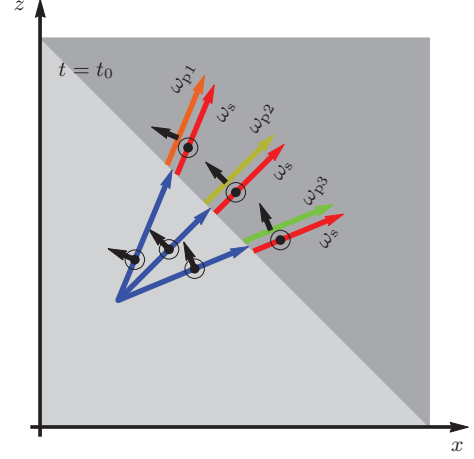

FIG. 3: Temporal frequency birefringence of the uniaxial inverse prism of Fig. 2. In a hybrid wave, the s-polarized and p-polarized parts experience ordinary (monochromatic) and extraordinary (polychromatic) temporal refraction, respectively.

uniaxial system of Fig. 2, taking the ratio of (3) and (2) yields

$$n_1 \omega_1 = \pm n_{\parallel} \omega_{\mathrm{s}}. \qquad (9)$$

This relation, illustrated in Fig. 3, may be considered as the *dual of Snell law* between isotropic media ($n_1 \sin\theta_1 = n_2 \sin\theta_2$): it is a transformation of temporal frequency (ω_1 to $\omega_2 = \omega_{\mathrm{s}}$), instead of spatial frequency or angle (θ_1 to θ_2), induced by a temporal interface, instead of a spatial interface, between two distinct media (n_1 and $n_2 = n_{\parallel}$). This corresponds to conventional time refraction or photon acceleration discussed in [2, 3], and we therefore refer to it here as *ordinary* temporal refraction law.

In the case of p-polarization, the temporal refraction relation, obtained by taking the ratio of (6b) to (2), enforcing $\mathbf{k}_1 = \mathbf{k}_2 = \mathbf{k}$, and writing $k_x = |\mathbf{k}|\cos(\theta)$ and $k_z = |\mathbf{k}|\sin(\theta)$, takes the more complex form

$$n_1 \omega_1 = \pm \frac{n_{\parallel} n_{\perp}}{\sqrt{n_{\parallel}^2 \cos^2(\theta) + n_{\perp}^2 \sin^2(\theta)}} \omega_{\mathrm{p}} = n(\mathbf{k})\omega_{\mathrm{p}}, \quad (10)$$

where θ is defined in the inset of Fig. 2(a). This relation, which is also illustrated in Fig. 3, is the *extraordinary* counterpart of (9), and may be considered as the *dual of Snell law* with an anisotropic medium.

Since it imparts different frequency jumps to s-polarized and p-polarized waves propagating in a given direction, as illustrated Fig. 3, the uniaxial inverse prism may be expected to induce unusual polarization transformation in the case of a hybrid (s- and p-polarized) wave. To investigate this, let us consider a plane wave that is linearly polarized in the $y-z$ plane, and hence p-s hybrid, and propagating along the x-axis in the earlier isotropic
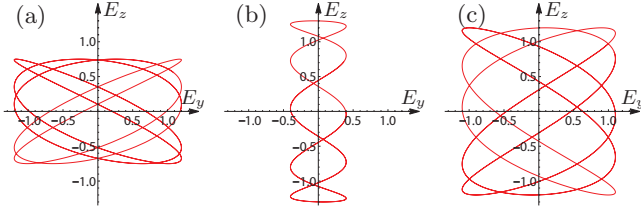
FIG. 4: Lissajous curve traced by tip of the electric field vector (Lissajous polarization) in the inverse prism of Fig. 2. (a) $A = 1.2$, $B = 0.75$, $\omega_s/c = 5$, $\omega_p/c = 4$, $\phi_y = -\pi/18$, and $\phi_z = -\pi/2$. (b) $A = 0.4$, $B = 1.3$, $\omega_s/c = 5$, $\omega_p/c = 1$, $\phi_y = -\pi/18$, and $\phi_z = \pi/2$. (c) $A = 1.1$, $B = 1.2$, $\omega_s/c = 5$, $\omega_p/c = 3$, $\phi_y = -\pi/18$, and $\phi_z = \pi/4$.

medium [see inset of Fig. 2(a)],

$$\mathbf{E}_1(x,t) = \mathbf{e}_y E_y \cos(k_x x - \omega_1 t) + \mathbf{e}_z E_z \cos(k_x x - \omega_1 t). \tag{11}$$

At the temporal interface, the y (s-polarized) component of the electric field undergoes the frequency shift ω_1 to ω_s (ordinary wave), while the z (p-polarized) component of the electric field undergoes the frequency shift ω_1 to ω_p (extraordinary wave). Moreover, as previously mentioned, each of the s and p component splits into transmitted and reflect waves with respective coefficients $T_\mathrm{p,s}$ and $R_\mathrm{p,s}$. Therefore, the wave transmitted ($+$) at the interface reads

$$\begin{aligned}\mathbf{E}_2^+(x,t) =&\mathbf{e}_y T_\mathrm{s} E_y \cos[k_x x - \omega_\mathrm{s}(t - t_0) - \omega_1 t_0] \\ &+ \mathbf{e}_z T_\mathrm{p} E_z \cos[k_x x - \omega_\mathrm{p}(t - t_0) - \omega_1 t_0],\end{aligned} \tag{12}$$

which may be alternatively written as

$$\mathbf{E}_2^+(x,t) = \mathbf{e}_y A \cos(\omega_\mathrm{s} t + \phi_y) + \mathbf{e}_z B \cos(\omega_\mathrm{p} t + \phi_z), \tag{13}$$

with $A = T_\mathrm{s} E_y$, $B = T_\mathrm{p} E_z$, $\phi_y = -k_x x - (\omega_\mathrm{s} - \omega_1)t_0$ and $\phi_z = -k_x x - (\omega_\mathrm{p} - \omega_1)t_0$.

Due to the different time-rate variations in its y component (ω_s) and z component (ω_p), the field (13) has a polarization response that is more complex than the usual elliptical polarization. Indeed, Equation (13) represents the parametric system, with parameter t,

$$\begin{aligned}E_{2y}^+(t) &= A \cos(\omega_\mathrm{s} t + \phi_x), \\ E_{2y}^+(t) &= B \cos(\omega_\mathrm{p} t + \phi_z),\end{aligned} \tag{14}$$

which describes Lissajous curves [25]. Thus, the tip of the electric field vector in (13) traces a Lissajous curve in space and time, and the inverse prism therefore transforms linear polarization into *Lissajous polarization*, represented in Fig. 4 for three different media parameter sets. Lissajous polarization is naturally a generalization of elliptic and circular polarizations, which occur here in the limit case of a later isotropic medium for which $\omega_\mathrm{s} = \omega_\mathrm{p}$ with $A \neq B$ and $A = B$, respectively.

Owing to the daily growing of demands for increasing the density of information carried through communication channels, the orbital and spin angular momentum of light have been considered as two degrees of freedom for modulating more amount of information into a twisted optical beam. After the renowned work by Allen and his colleagues in 1992 [26], there have been an extensive amount theoretical and experimental research done on different aspects of angular momentum of light [27–34]. Now the property of the temporal interface to produce Lissajous harmonic patterns calls for an extended study on the spin-orbital interaction of light at the space-time modulated interfaces, among which the temporal interface is a special case. More specifically, one can examine how the temporal interface may affect the orbital and angular momentum of a structured beam, e.g. Laguerre-Gaussian beam, and its inherent vortices. Furthermore, by using the standard Minkowski diagrams, as shown in detail in [24], one can extend the study to the subluminally and superluminally modulated space-time interfaces, although the mathematics would be more complicated. We believe that such an extending studies on the angular momentum of light would definitely lead to more subtle results and help the scientific community achieve a skill set to dynamically manipulate the spin-orbital angular momentum of light beams.

In this letter, we introduced a uniaxial temporal dielectric medium, which essentially maps the wave vector domain into the frequency domain and offers the inverse operation of conventional prisms. On account of the general space-time duality and by swapping the broken spatial symmetry and temporal frequency dispersion of a prism with their counterparts, i.e. broken temporal symmetry and spatial frequency dispersion, we achieved the inverse prism medium and we showed the corresponding directional polychromatic frequency generation. Furthermore, we showed that due to the uniaxial nature of inverse prism, the frequency refraction at its interface is birefringent for a hybrid wave and we added the extraordinary version of Snell's law of frequency refraction to the previously reported ordinary version. Finally, we showed that the inverse prism affects the polarization of a hybrid wave in an interesting manner and we introduced a new type of polarization, Lissajous polarization, which may be exploited for manipulation of spin-orbital angular momentum of light.

* Electronic address: alireza.akbarzadeh@polymtl.ca

[1] I. Newton, *Opticks; Or, a Treatise of the Reflections, Refractions, Inflections and Colours of Light* (William and John Innys, 1721).

[2] J. Mendonça, A. Guerreiro, and A. M. Martins, Phys. Rev. A **62**, 033805 (2000).

[3] J. T. Mendonça, *Theory of Photon Acceleration* (CRC Press, 2000).

[4] D. K. Kalluri, *Electromagnetics of Time Varying Complex Media: Frequency and Polarization Transformer*

(CRC Press, 2016).

[5] A. B. Shvartsburg, Phys. Usp. **48**, 797 (2005).

[6] D. Kaup, A. Reiman, and A. Bers, Rev. Mod. Phys. **51**, 275 (1979).

[7] E. J. Reed, M. Soljačić, and J. D. Joannopoulos, Phys. Rev. Lett. **90**, 203904 (2003).

[8] E. J. Reed, M. Soljačić, and J. D. Joannopoulos, Phys. Rev. Lett. **91**, 133901 (2003).

[9] S. Taravati and C. Caloz, IEEE Trans. Antennas Propag. **65**, 442 (2017).

[10] F. R. Morgenthaler, IRE Trans. on Microw. Theory and Tech. **6**, 167 (1958).

[11] L. Felsen and G. Whitman, IEEE Trans. Antennas and Propag. **18**, 242 (1970).

[12] R. L. Fante, IEEE Trans. Antennas Propag. **19**, 417 (1971).

[13] Y. Xiao, D. N. Maywar, and G. P. Agrawal, J. Opt. Soc. Am. B **28**, 1685 (2011).

[14] Y. Xiao, G. P. Agrawal, and D. N. Maywar, Opt. Lett. **36**, 505 (2011).

[15] Y. Xiao, D. N. Maywar, and G. P. Agrawal, Opt. Lett. **39**, 574 (2014).

[16] B. Plansinis, W. Donaldson, and G. Agrawal, Phys. Rev. Lett. **115**, 183901 (2015).

[17] M. F. Yanik and S. Fan, Phys. Rev. Lett. **93**, 173903 (2004).

[18] N. Chamanara and C. Caloz, Phys. Rev. B **94**, 075413 (2016).

[19] Y. Hadad, D. Sounas, and A. Alu, Phys. Rev. B **92**, 100304 (2015).

[20] M. Born and E. Wolf, *Principles of Optics: Electromagnetic Theory of Propagation, Interference and Diffraction of Light* (Elsevier, 2013).

[21] J. A. Kong, *Theory of Electromagnetic Waves* (Wiley-Interscience, 1975).

[22] M. G. Silveirinha, Phys. Rev. B **75**, 115104 (2007).

[23] F. Biancalana, A. Amann, A. V. Uskov, and E. P. Oreilly, Phys. Rev. E **75**, 046607 (2007).

[24] Z.-L. Deck-Léger, A. Akbarzadeh, and C. Caloz, arXiv preprint arXiv:1611.01366 (2017).

[25] L. Surhone, M. Timpledon, and S. Marseken, *Lissajous Curve: Mathematics, Parametric Equation, Curve, Nathaniel Bowditch, Jules Antoine Lissajous, Ellipse, Parabola, Line, Circle, Radian, Rational Number* (Betascript Publishing, 2010).

[26] L. Allen, M. W. Beijersbergen, R. Spreeuw, and J. Woerdman, Phys. Rev. A **45**, 8185 (1992).

[27] L. Allen, M. Padgett, and M. Babiker, Progress in Optics **39**, 291 (1999).

[28] K. Y. Bliokh and Y. P. Bliokh, Phys. Rev. Lett. **96**, 073903 (2006).

[29] K. Y. Bliokh, A. Niv, V. Kleiner, and E. Hasman, Nat. Photonics **2**, 748 (2008).

[30] K. Y. Bliokh, M. A. Alonso, E. A. Ostrovskaya, and A. Aiello, Phys. Rev. A **82**, 063825 (2010).

[31] K. Y. Bliokh, A. Y. Bekshaev, and F. Nori, arXiv preprint arXiv:1308.0547 (2013).

[32] K. Y. Bliokh, D. Smirnova, and F. Nori, Science **348**, 1448 (2015).

[33] K. Y. Bliokh, F. Rodríguez-Fortuño, F. Nori, and A. V. Zayats, Nat. Photonics **9**, 796 (2015).

[34] K. Y. Bliokh, C. Samlan, C. Prajapati, G. Puentes, N. K. Viswanathan, and F. Nori, Optica **3**, 1039 (2016).